Available online at www.sciencedirect.com
ScienceDirect
Ceramics International 35 (2009) 3147–3151
CERAMICS INTERNATIONAL
www.elsevier.com/locate/ceramint

Rapid consolidation of nanocrystalline Al_2O_3 reinforced Ni–Fe composite from mechanically alloyed powders by high frequency induction heated sintering

Na-Ra Park [a], Dong-Mok Lee [a], In-Yong Ko [a], Jin-Kook Yoon [b], In-Jin Shon [a,c,*]

[a] Division of Advanced Materials Engineering and the Research Center of Industrial Technology, Engineering College, Chonbuk National University, Chonbuk 561-756, Republic of Korea
[b] Advanced Functional Materials Research Center, Korea Institute of Science and Technology, PO Box 131, Cheongryang, Seoul 130-650, Republic of Korea
[c] Department of Hydrogen and Fuel Cells Engineering, Specialized Graduate School, Chonbuk National University, Chonbuk 561-756, Republic of Korea

Received 18 February 2009; received in revised form 9 April 2009; accepted 3 May 2009
Available online 6 June 2009

Abstract

Nano-powders of Ni–Fe and Al_2O_3 were made from NiO and FeAl powders by high-energy ball milling. Nanocrystalline $5Ni_{0.6}Fe_{0.4}$–Al_2O_3 composite was consolidated by high frequency induction heated sintering (HFIHS) method within 2 min from mechanically alloyed powders of Al_2O_3 and Ni–Fe. The average grain size and mechanical properties of the composite were investigated.

Keywords: B. Composite; C. Mechanical properties; Rapid sintering; Nanophase; NiFe-Al_2O_3

1. Introduction

The continuous increase in the performance requirement of materials for aerospace and automotive applications have lead to development of several structural composite materials. Among these, metal matrix composites refer to a kind of material in which rigid ceramic reinforcements are embedded in a ductile metal or alloy matrix. Metal matrix composites combine metallic properties (ductility and toughness) with ceramic characteristics (high strength and modulus), leading to greater strength in shear and compression and to higher service temperature capabilities. The attractive physical and mechanical properties that can be obtained with metal matrix composites, such as high specific modulus, strength-to-weigh ratio, fatigue strength, and temperature stability and wear resistance, have been documented extensively [1–5].

Traditionally, discontinuously reinforced metal matrix composites have been produced by several processing routes such as powder metallurgy, spray deposition, mechanical alloying, various casting techniques and SHS (self-propagating high temperature synthesis). One of all these techniques, high-energy ball milling and mechanical alloying of powder mixtures, were reported to be efficient techniques for the preparation of nanocrystalline metals and alloys, which is a combination of mechanical milling and chemical reactions [6].

Nanocrystalline materials have received much attention as advanced engineering materials with improved physical and mechanical properties [7,8]. As nanomaterials possess high strength, high hardness, excellent ductility and toughness, undoubtedly, more attention has been paid for the application of nanomaterials [9,10]. In recent days, nanocrystalline powders have been developed by the thermochemical and thermo-mechanical process named as the spray conversion process (SCP), co-precipitation and high-energy milling [11–13]. However, the grain size in sintered materials becomes much larger than that in pre-sintered powders due to a fast grain growth during conventional sintering process. Therefore, even though the initial particle size is less than 100 nm, the grain size increases rapidly up to 500 nm or larger during the conventional

* Corresponding author at: Division of Advanced Materials Engineering and the Research Center of Industrial Technology, Engineering College, Chonbuk National University, Chonbuk 561-756, Republic of Korea. Tel.: +82 63 2381; fax: +82 63 270 2386.
E-mail address: ijshon@chonbuk.ac.kr (I.-J. Shon).

0272-8842/$36.00
doi:10.1016/j.ceramint.2009.05.006

sintering [14]. So, controlling grain growth during sintering is one of the keys to the commercial success of nanostructured materials. In this regard, the high frequency induction activated sintering method which can make dense materials within 2 min, has been shown to be effective in achieving this goal [15,16].

The purpose of this work is to produce dense nanocrystalline Al_2O_3 reinforced Ni–Fe composite within 2 min from mechanically alloyed powders by using this high frequency induction activated sintering method and to evaluate its mechanical properties (hardness and fracture toughness).

2. Experimental procedure

Powders of 99% NiO (−325 mesh, Alfa) and 99% pure FeAl (<200 μm, Sinagigong, Inc) were used as a starting materials. 3NiO and 2FeAl powder mixtures were first milled in a high-energy ball mill, Pulverisette-5 planetary mill with 250 rpm and for 10 h. Tungsten carbide balls (8.5 mm in diameter) were used in a sealed cylindrical stainless steel vial under argon atmosphere. The weight ratio of ball-to-powder was 30:1. Milling resulted in a significant reduction of grain size. The grain sizes of Ni–Fe alloy and Al_2O_3 were calculated by C. Suryanarayana and M. Grant Norton's formula [17],

$$B_r(B_{crystalline} + B_{strain})\cos\theta = \frac{k\lambda}{L} + \eta\sin\theta \quad (1)$$

where B_r is the full width at half-maximum (FWHM) of the diffraction peak after instrument correction; $B_{crystalline}$ and B_{strain} are FWHM caused by small grain size and internal stress, respectively; k is constant (with a value of 0.9); λ is wavelength of the X-ray radiation; L and η are grain size and internal strain, respectively; and θ is the Bragg angle. The parameters B and B_r follow Cauchy's form with the relationship: $B = B_r + B_s$, where B and B_s are FWHM of the broadened Bragg peaks and the standard sample's Bragg peaks, respectively.

After milling, the mixed powders were placed in a graphite die (outside diameter, 45 mm; inside diameter, 20 mm; height, 40 mm) and then introduced into the pulsed current activated sintering system made by Eltek in South Korea, shown schematically in Fig. 1. The four major stages in the synthesis are as follows. Stage 1: Evacuation of the system. Stage 2: Application of uniaxial pressure. Stage 3: Heating of sample by induced current. Stage 4: Cooling of sample. The process was carried out under a vacuum of 40 mTorr.

The relative densities of the synthesized sample measured by the Archimedes method are over 95% of the theoretical value.

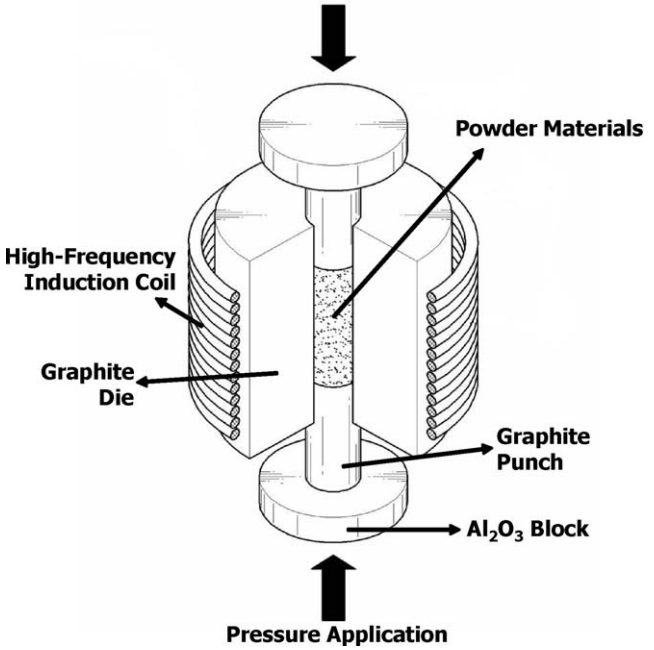

Fig. 1. Schematic diagram of the apparatus for high-frequency induction heated sintering.

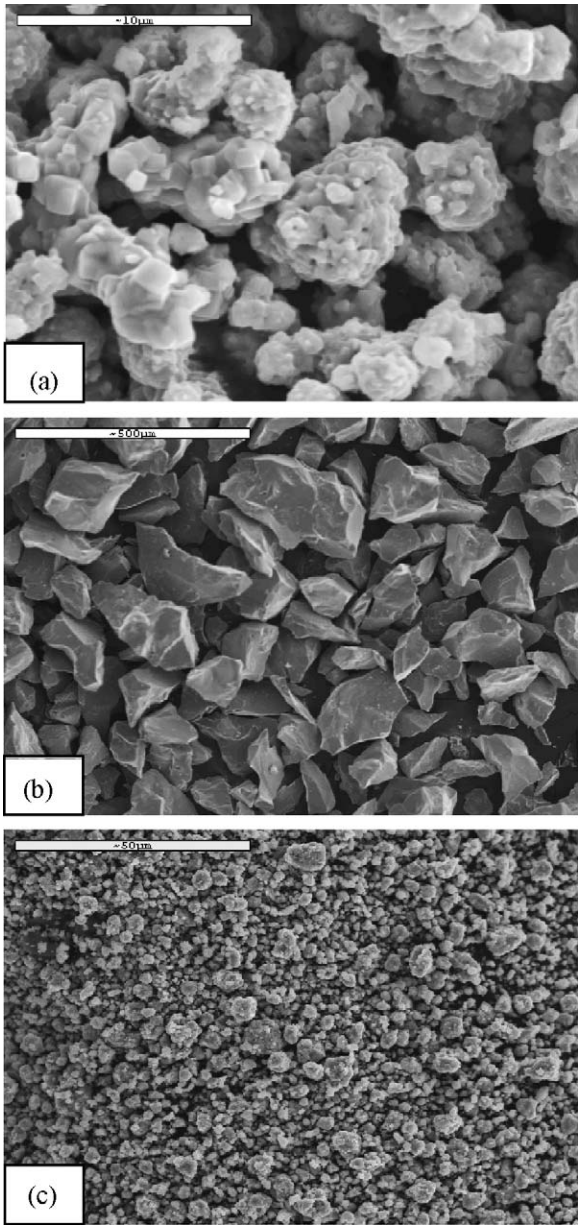

Fig. 2. Scanning electron microscope images of raw materials and milled powder: (a) NiO, (b) FeAl and (c) milled powder.

Microstructural information was obtained from product samples which were polished at room temperature. Compositional and micro structural analyses of the products were made through X-ray diffraction (XRD) and scanning electron microscopy (SEM) with energy dispersive X-ray analysis (EDAX). Vickers hardness was measured by performing indentations at load of 50 kg and a dwell time of 15 s on the synthesized samples.

3. Results and discussion

Fig. 2 shows the SEM images of the raw materials and milled powder used. Milling resulted in a significant reduction of grain size. X-ray diffraction result of high-energy ball milled powders is shown in Fig. 3(c). The reactant powders of NiO and Al were not detected but products, Ni–Fe alloy and Al_2O_3, were detected. From the above result the mechanical alloy occurs completely during the milling. The net reaction can be considered to be a combination of the following two reactions:

$$3NiO + 2Al \rightarrow 3Ni + Al_2O_3 \quad (2)$$

$$3Ni + 2Fe \rightarrow 5Ni_{0.6}Fe_{0.4} \quad (3)$$

Reaction Eq. (2) is the well-known, exothermic reaction, for which the standard enthalpy of reaction ranges from −964.46 to

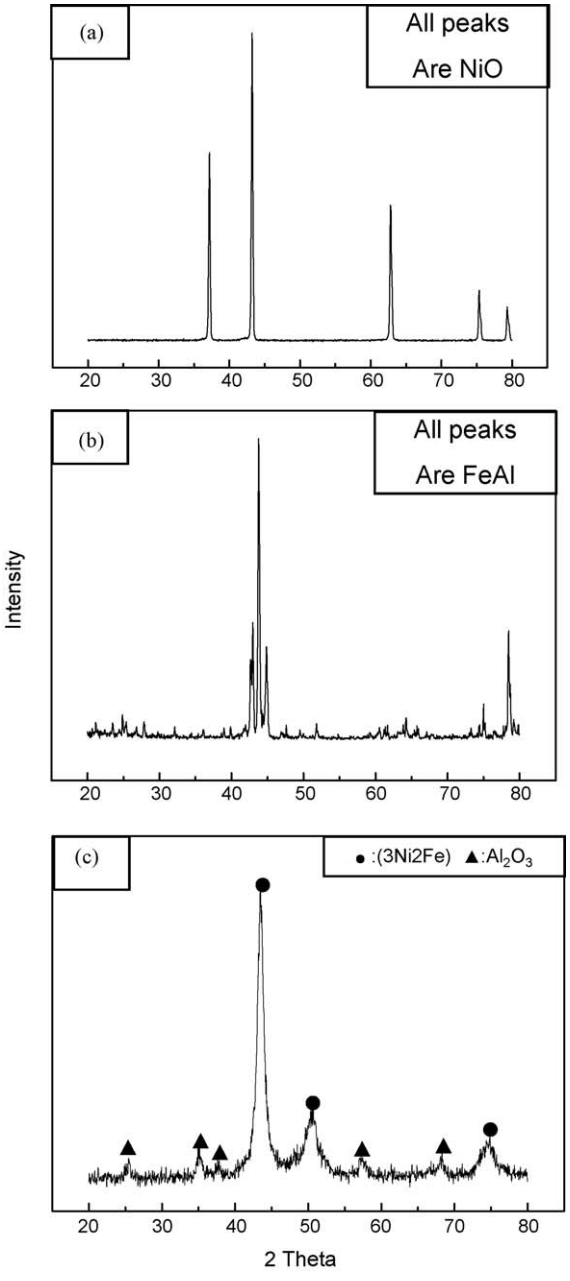

Fig. 3. XRD patterns of raw materials and mechanically alloyed powder: (a) NiO, (b) FeAl and (c) milled 3NiO-2FeAl.

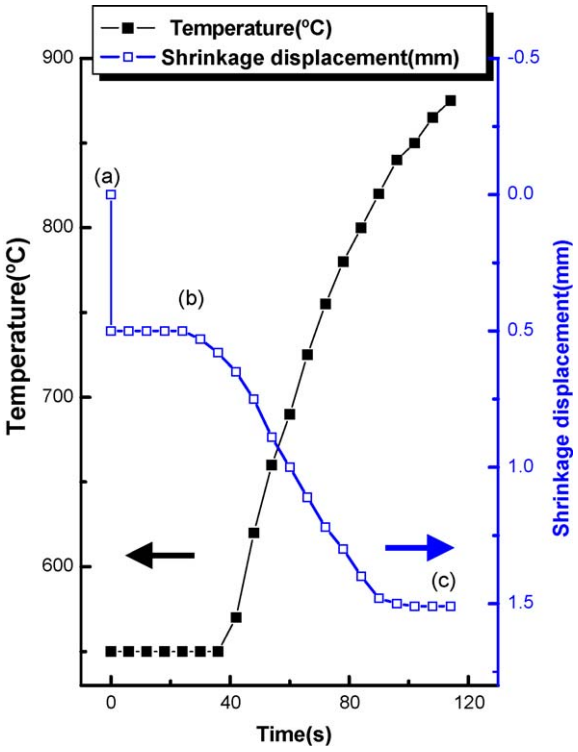

Fig. 4. Variation of temperature and shrinkage displacement with heating time during high frequency induction heated sintering of $5Ni_{0.6}Fe_{0.4} + Al_2O_3$.

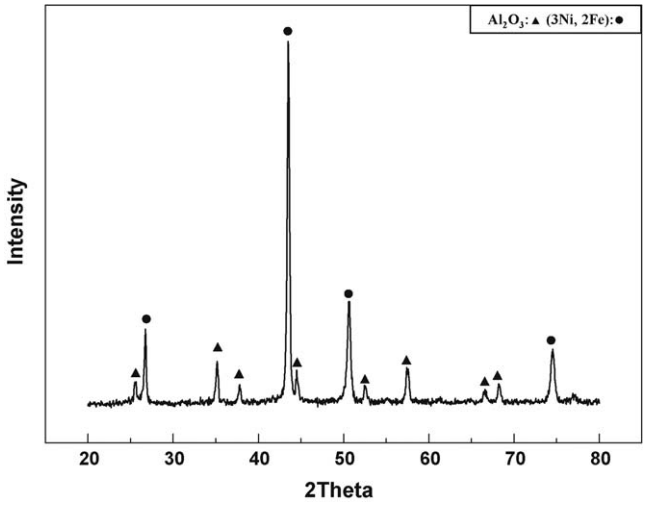

Fig. 5. XRD patterns of the $5Ni_{0.6}Fe_{0.4}$–Al_2O_3 composite heated to 900 °C.

−989.409 kJ over the temperature range of 700 °C (just above the melting temperature of Al, 660 °C) to 1400 °C (just below the melting point of Ni, 1455 °C).

The FWHM value obtained from XRD pattern of the milled powder is larger than that of raw powder due to an internal strain and a reduction of grain size. The average grain sizes of Ni–Fe and Al_2O_3 measured by C. Suryanarayana and M. Grant Norton's formula are about 40 nm and 25 nm, respectively.

The variations in shrinkage displacement and temperature of the surface of the graphite die with heating time during the processing of Ni–Fe and Al_2O_3 system are shown Fig. 4. As the induced current was applied the specimen showed the shrinkage displacement slowly increased with temperature up to about 550 °C, but then abruptly increased at about 600 °C. X-ray diffraction pattern of sample heated to 880 °C is shown in Fig. 5. Ni–Fe alloy and Al_2O_3, were detected. The structure parameters, i.e. the average grain sizes of Ni–Fe alloy and Al_2O_3 are obtained from the X-ray data by C. Suryanarayana and M. Grant Norton's formula, were 165 nm and 58 nm, respectively. Fig. 6 shows the BSE (back scattered electron) image of sample heated to 900 °C and X-ray mappings. The Al_2O_3 particles with dark color were well distributed in matrix (Ni–Fe alloy with grey color), ascertained by BSE image and X-ray mapping of shown in Fig. 6.

Vickers hardness measurements were made on polished sections of the $5Ni_{0.6}Fe_{0.4}$–Al_2O_3 composite using a 50 kg_f load and 15 s dwell time. The calculated hardness value of $5Ni_{0.6}Fe_{0.4}$–Al_2O_3 composite was 740 kg/mm^2. This value represents an average of five measurements. Indentations with large enough loads produced median cracks around the indent. The length of these cracks permits an estimation of the fracture toughness of the material by Niihara et al. expression [18,19].

$$K_{IC} = 0.023\left(\frac{c}{a}\right)^{-3/2} \cdot H_v \cdot a^{1/2} \quad (3)$$

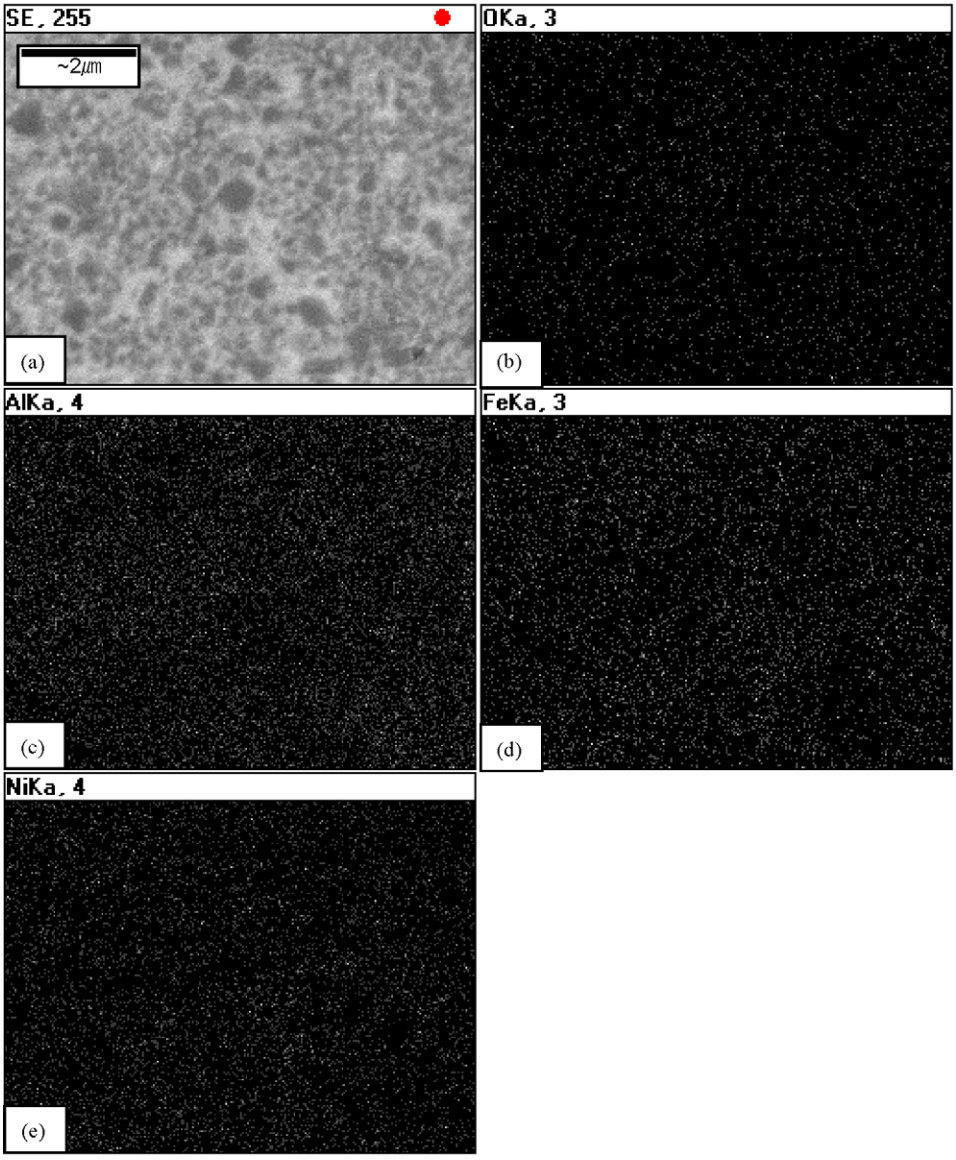

Fig. 6. Scanning electron microscope image and X-ray mapping of $5Ni_{0.6}Fe_{0.4}$–Al_2O_3 composite: (a) SEM image, (b) oxygen mapping, (c) aluminum mapping, (d) iron mapping, (e) nickel mapping.

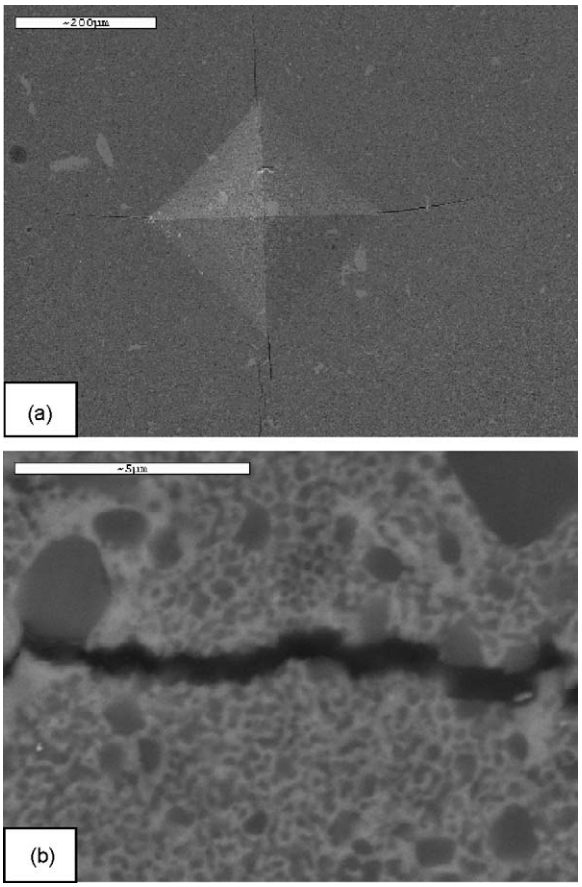

Fig. 7. (a) Vickers hardness indentation and (b) median crack propagating of $5Ni_{0.6}Fe_{0.4}$–Al_2O_3 composite.

where c is the trace length of the crack measured from the center of the indentation, a the half of average length of two indent diagonals, and H_v the hardness.

The calculated fracture toughness value of $5Ni_{0.6}Fe_{0.4}$–Al_2O_3 composite is about 8 MPa $m^{1/2}$. As in the case of hardness value, the toughness value is the average of measurements on five measurements. A typical indentation pattern for $5Ni_{0.6}Fe_{0.4}$–Al_2O_3 composite is shown in Fig. 7. Typically, one to three additional cracks were observed to propagate from the indentation corner. A higher magnification view of the indentation median crack in the composite is shown in Fig. 7(b). This shows the crack deflected at Al_2O_3 phase. The absence of reported values for hardness and toughness on $5Ni_{0.6}Fe_{0.4}$–Al_2O_3 composite precludes making direct comparison to the results obtained in this work to show the influence of grain size.

4. Conclusions

Nano-powders of Ni–Fe and Al_2O_3 were made from NiO and FeAl powders by high-energy ball milling. Using the high frequency induction activated sintering method, the densification of nanostructured $5Ni_{0.6}Fe_{0.4}$–Al_2O_3 composite was accomplished from mechanically alloyed powders. Complete densification can be achieved within duration of 2 min. The relative density of the composite was 95.5% for the applied pressure of 80 MPa and the induced current. The average grain sizes of Ni–Fe alloy and Al_2O_3 prepared by HFIHS were about 165 nm and 58 nm, respectively. The average hardness and fracture toughness values obtained were 740 kg/mm^2 and 8 MPa $m^{1/2}$, respectively.

Acknowledgement

This paper was supported by the selection of research-oriented professor of Chonbuk National University in 2009.

References

[1] L. Ceschini, G. Minak, A. Morri, Tensile and fatigue properties of the AA6061/20 vol% Al_2O_3p and AA7005/10 vol% Al_2O_3p composites, Compos. Sci. Technol. 66 (2) (2006) 333–342.
[2] S.C. Tjong, Z.Y. Ma, Microstructural and mechanical characteristics of in situ metal matrix composites, Mater. Sci. Eng. 29 (2000) 49–113.
[3] D.J. Lloyd, Particle reinforced aluminum and magnesium metal matrix composites, Int. Mater. Rev. 39 (1) (1994) 1–45.
[4] J.M. Torralba, F. Velasco, P/M aluminum matrix composites: an overview, J. Mater. Proc. Tech. 133 (1–2) (2006) 203–206.
[5] R. Fan, B. Liu, J. Zhang, J. Bi, Y. Yin, Kinetic evaluation of combustion synthesis $3TiO_2 + 7Al \rightarrow 3TiAl + 2Al_2O_3$ using non-isothermal DSC method, Mater. Chem. Phys. 91 (1) (2005) 140–145.
[6] S. Paris, E. Gaffet, F. Bernard, Z.A. Munir, Spark plasma synthesis from mechanically activated powders: a versatile route for producing dense nanostructured iron aluminides, Scripta Mater. 50 (5) (2004) 691–696.
[7] M.S. El-Eskandarany, Structure and properties of nanocrystalline TiC full-density bulk alloy consolidated from mechanically reacted powders, J. Alloys Compd. 305 (1–2) (2000) 225–238.
[8] L. Fu, L.H. Cao, Y.S. Fan, Two-step synthesis of nanostructured tungsten carbide-cobalt powders, Scripta Mater. 44 (7) (2001) 1061–1068.
[9] E.T. Thostenson, C. Li, T.W. Chou, Nanocomposites in context, Compos. Sci. Technol. 65 (2005) 491–516.
[10] S. Berger, R. Porat, R. Rosen, Nanocrystalline materials: a study of WC-based hard metals, Prog. Mater. Sci. 42 (1–4) (1997) 311–320.
[11] I.J. Shon, H.K. Park, H.C. Kim, J.K. Yoon, K.T. Hong, I.Y. Ko, One-step synthesis and densification of nanostructured TiSi2–SiC composite from mechanically activated (TiC + 3Si) powders by high-frequency-induced heated combustion, Scripta Mater. 56 (8) (2007) 665–668.
[12] Z. Fang, J.W. Eason, Study of nanostructured WC-Co composites, Int. J. Refract. Met. Hard Mater. 13 (5) (1995) 297–303.
[13] A.I.Y. Tok, L.H. Luo, F.Y.C. Boey, Carbonate co-precipitation of Gd_2O_3-doped CeO2 solid solution nano-particles, Mater. Sci. Eng. A 383 (2) (2004–2005) 229–234.
[14] M. Sommer, W.D. Schubert, E. Zobetz, P. Warbichler, On the formation of very large WC crystals during sintering of ultrafine WC–Co alloys, Int. J. Refract. Met. Hard Mater. 20 (1) (2002) 41–50.
[15] H.C. Kim, I.J. Shon, I.J. Jeong, I.Y. Ko, J.K. Yoon, J.M. Doh, Rapid sintering of ultra fine WC and WC-Co hard materials by high-frequency induction heated sintering and their mechanical properties, Met. Mater. Int. 13 (2007) 39–46.
[16] H.C. Kim, I.J. Shon, I.K. Jeong, I.Y. Ko, Rapid sintering of nanocrystalline 8 mol.%Y2O3-stabilized ZrO2 by high-frequency induction heating method, Met. Mater. Int. 12 (2006) 393–399.
[17] C. Suryanarayana, M. Grant Norton, X-ray Diffraction A Practical Approach, Plenum Press, New York, 1998, p. 207.
[18] K. Niihara, R. Morena, D.P.H. Hasselman, Evaluation of KIC of brittle solids by the indentation method with low crack-to-indent ratios, J. Mater. Sci. Lett. 1 (1982) 12–16.
[19] D.Y. Oh, H.C. Kim, J.K. Yoon, I.J. Shon, One step synthesis of dense MoSi2–SiC composite by high-frequency induction heated combustion and its mechanical properties, J. Alloys Compd. 395 (1–2) (2005) 174–180.